The Effect of Soil-Vegetation-Atmosphere Interaction on Slope Stability: A Numerical Study

Jamalinia, Elahe; Vardon, Phil; Steele-Dunne, Susan

DOI
10.1680/jenge.18.00201

Publication date
2019

Document Version
Final published version

Published in
Environmental Geotechnics

Citation (APA)
Jamalinia, E., Vardon, P., & Steele-Dunne, S. (2019). The Effect of Soil-Vegetation-Atmosphere Interaction on Slope Stability: A Numerical Study. *Environmental Geotechnics*, *8*(7), 430-441. https://doi.org/10.1680/jenge.18.00201

Cite this article
Jamalinia E, Vardon PJ and Steele-Dunne SC
The effect of soil–vegetation–atmosphere interaction on slope stability: a numerical study.
Environmental Geotechnics,
https://doi.org/10.1680/jenge.18.00201

Research Article
Paper 1800201
Received 14/12/2018; Accepted 23/08/2019

Keywords: geotechnical engineering/
seepage/slopes – stabilization

Environmental Geotechnics

ice Publishing

The effect of soil–vegetation–atmosphere interaction on slope stability: a numerical study

1 **Elahe Jamalinia** BSc, MSc
PhD Researcher, Faculty of Civil Engineering and Geosciences, Delft University of Technology, Delft, the Netherlands (corresponding author: e.jamalinia@tudelft.nl) (Orcid:0000-0002-1874-2315)

2 **Philip J. Vardon** MEng, PhD
Associate Professor, Faculty of Civil Engineering and Geosciences, Delft University of Technology, Delft, the Netherlands (Orcid:0000-0001-5614-6592)

3 **Susan C. Steele-Dunne** BSc, MSc, PhD
Professor, Faculty of Civil Engineering and Geosciences, Delft University of Technology, Delft, the Netherlands (Orcid:0000-0002-8644-3077)



The stability of a dike is influenced strongly by its water content, by way of changes in effective stress and weight. While flow through porous media is relatively well understood, water flux in and out of a dike through a vegetated surface is not as well understood. This paper presents a numerical study of the soil–vegetation–atmosphere interaction and discusses how it influences the stability of dikes covered with grass. A crop model was used to simulate vegetation growth and infiltration in response to meteorological forcing. The PLAXIS finite-element method model was used to simulate the impact of this infiltration on hydromechanical behaviour and dike stability. Results from a 4-year analysis indicated a strong correlation between root zone water content (WC_{rz}) and factor of safety, although the relationship is not unique. The leaf area index (*LAI*) was also found to have a strong, lagged correlation with the water flux into the dike. This suggests that monitoring *LAI* could be a useful tool to identify vulnerable locations along dikes. It is therefore proposed that vegetation and root zone water content could be used as an indication to detect vulnerable dikes in the early stage.

Notation

c	soil cohesion
c_{input}	input cohesion
$c_{reduced}$	reduced cohesion
D_L	drainage from the root zone in the crop model
D_P	drainage from the root zone in one-dimensional geotechnical model
D_{rate}	maximum drainage rate
$d_{M\ root}$	maximum root length
E	Young's modulus
e_{int}	initial void ratio
FoS	factor of safety
$f_{(lv)}$	fraction of dry vegetation matter to leaves
$\boldsymbol{g}$	vector of gravitational acceleration
h	suction
k_{rel}	relative permeability
k_{sat}	saturated hydraulic conductivity
k_{sat}	saturated hydraulic conductivity matrix
In	leaf interception
LAI	leaf area index
LAI_c	remaining leaf area index after cutting
LAI_{cr}	critical leaf area for internal shading effect
P	precipitation
p_{wp}	pore water pressure
Q_{net}	surface boundary net flux
$\boldsymbol{q}$	vector of specific discharge
Rn	run-off
SLA	specific leaf area
WC_{body}	dike body water content
WC_{rz}	root zone water content
α, n, m	soil water characteristic curve fitting parameters
ΔLAI_d	death rate of leaf area
ΔW	growth rate of crop dry matter
ΔWA	daily changes in the amount of water stored in the root zone
γ_{sat}	saturated unit weight
θ	water content
θ_{cr}	critical water content
θ_{fc}	water content at field capacity
θ_r	residual water content
θ_{sat}	water content at saturation
θ_{wp}	water content at the wilting point
ρ_w	water density
ϕ	friction angle
ϕ_{input}	input friction angle
$\phi_{reduced}$	reduced friction angle
ψ	dilatancy angle

Introduction

Dikes are predominantly earth structures, whose primary objective is to provide protection against flood events along coasts, rivers and artificial waterways (CIRIA *et al.*, 2013). In the Netherlands, dikes are typically covered by clay and reinforced by grass. This provides an effective covering to the construction, protecting from soil erosion, particularly for river dikes (TAW, 1996). The surface is the most dynamic portion of a dike, as it is affected by atmospheric conditions – for example, rain, evaporation and transpiration (Franzluebbers, 2011). Soil–vegetation–atmosphere (SVA) interaction refers to the process in which atmospheric conditions influence both vegetation and soil states.

Vegetation growth and health are influenced by the ground: soil texture, nutrient availability, hydraulic properties and moisture availability. They also depend on climatic conditions: precipitation, radiation and temperature. A recent study from Vardon (2015) identified the major climatic variations expected to influence geotechnical infrastructure: increasing temperature (causing soil drying), increasing mean rainfall (causing reduction in soil suctions), increasing drought events (leading to drying and soil desiccation) and increasing intense precipitation (causing soil erosion, flooding and hydromechanical failure).

Dike inspectors conduct visual inspections of the dike surface, including vegetation, in order to identify deterioration or damage. Recent studies have highlighted the value of using vegetation condition as an indicator of subsurface conditions. For instance, Hasan *et al*. (2013) concluded that grass growing over areas with cracks and fractures was stressed due to a lack of moisture compared with grass over other areas. They noted that during winter and early spring, grass was stressed or dying in cracked areas, while it grew green in adjacent areas.

According to the Dutch Guidelines (Digigids, 2016), vegetation is one of the factors that dike inspectors should evaluate in their observation, by which the vegetation quality for each location is assessed and classified as good, medium, poor or bad (Cundill, 2016). However, these definitions are neither well-defined nor specific. Using vegetation indices would provide a more objective and quantitative indicator. Furthermore, using earth observation data – that is, remote sensing – to map vegetation indices facilitates large-scale monitoring and can be used to identify areas of interest for further investigation.

Few studies have investigated the impact of vegetation on the water fluxes into dikes and its consequential effect on stability – for example, studies by Hemmati *et al*. (2012), Tsiampousi *et al*. (2016), Rahardjo *et al*. (2013) and Elia *et al*. (2017). This study aims to bridge this gap by investigating the effect of vegetation in dike analysis assuming a typical regional dike covered with grass. Here it is hypothesised that vegetation and the surface layer of the soil act as a hydraulic buffer to the rest of the dike. Furthermore, vegetation responds to water content variations in the root zone, leading to the possibility of using it as a dike health indicator. In the current paper, a crop growth model is coupled to a geotechnical model to enable the investigation of SVA interaction due to the climatic conditions. The changes in the stability of a conceptional dike, based on the geometry and materials of a regional dike in the Netherlands, is investigated. In this initial study, cracking and desiccation of soil are not included, but a proposed approach offers the opportunity to do so in a further study.

Method

The system of interest is an idealised regional dike. The cross section is illustrated in Figure 1. The dike is 2 m high and 41 m wide, and the water levels on the left and right sides are 3 and 2·6 m, respectively. The dike's surface is vegetated with a permanent root zone depth of 40 cm extended over the surface layer (red area in Figure 1).

The modelling strategy is as follows: (*a*) a one-dimensional (1D) crop model is used to simulate the infiltration of water into and out of the root zone. This model uses weather data as input and calculates the evaporation, transpiration, water interception by the vegetation, drainage from the root zone layer and vegetation growth. (*b*) A 1D geotechnical model is used to simulate the hydraulic behaviour of the root zone, where only the calculated water in step (*a*) entering the root zone is applied as a top boundary condition. The hydraulic material properties of the root zone are optimised so that the drainage from the bottom of the root zone matches in both models. (*c*) A two-dimensional (2D) geotechnical model is used to simulate the hydromechanical behaviour in time, including both the displacement and the factor of safety (*FoS*). An overview of this process is given in the flow chart in Figure 2.

There are then three boundaries of interest in Figure 1: (*a*) the soil surface; (*b*) the bottom of the root zone (top of the dike body), which represents the coupling interface between the crop model

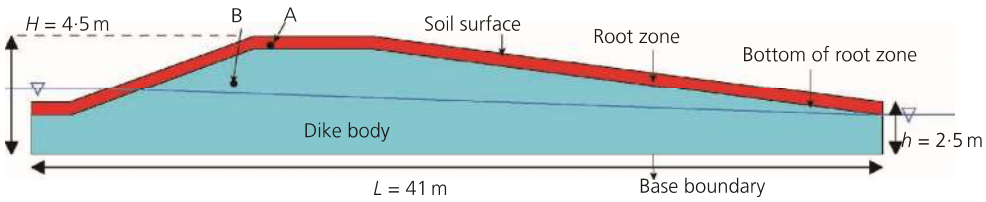

Figure 1. Geometry representing boundary, root zone layers and points in which results are plotted

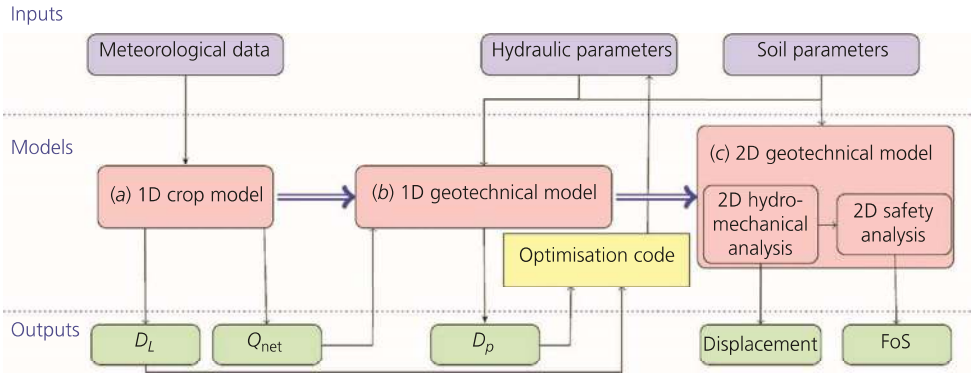

Figure 2. Flow chart for the numerical solution procedure

and the geotechnical model; and (*c*) the base boundary of the dike that is assumed to be impermeable. Results are plotted at points A and B during the analyses, which are representative locations in the root zone and the dike body. The phreatic surface is calculated in the geotechnical model. The vadose zone is of limited thickness and consists mainly of the root zone.

Crop model

The Lingra (Lintul Grassland) (Schapendonk *et al*., 1998) model is used for simulating the processes governing infiltration from the surface layer in response to climatic conditions and the consequential vegetation growth. Lingra was designed for applications such as yield forecasting, quantitative land-use evaluation and investigation of the effects of climate change on grass yields (Schapendonk *et al*., 1998). This model is based on the Lintul (Light Interception and Utilization simulator) concept as proposed by Spitters (1987). Lingra is specifically for grass growth, and the model can account for growth in water-limited conditions, which is the case for the grass on dikes. The main components of interest are the water balance and leaf growth. A more complete description of the model is provided by Shibu *et al*. (2010) and Bouman *et al*. (1996a).

Water balance equation

Lingra solves a 1D mass balance equation in the root zone using a tipping bucket approach (Bouman *et al*., 1996a). The soil water balance is calculated for the root zone layer (Figure 3), whose thickness increases with downward root elongation and has a predefined water storage capacity (Shibu *et al*., 2010).

The daily changes in the amount of water stored in the root zone, ΔWA, is calculated from the 'effective precipitation' (precipitation (P) minus interception (In)), minus bare soil evaporation (E) and transpiration (T) (collectively referred to as evapotranspiration, ET), minus drainage (D_L) and run-off (Rn):

$$1. \quad \Delta WA = P - In - ET - D_L - Rn$$

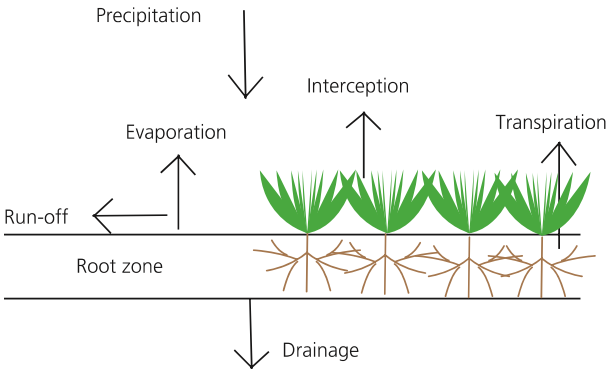

Figure 3. Root zone water balance in Lingra

All quantities are in metres per day. The interception and evapotranspiration are dependent on the amount of vegetation, quantified as the leaf area index (LAI, m^2 leaf/m^2 ground). When the amount of water in the root zone reaches the field capacity, the excess water drains from the lower boundary of the root zone. This drainage flux (D_L) is limited by the maximum drainage rate (D_{rate}) of the subsoil. Additional water leaves as run off (Rn). In this crop model, upward water flow (capillary rise) is disregarded and lateral influx or outflux of water is not considered (Bouman *et al*., 1996a). However, in the geotechnical model, these fluxes are included.

Leaf growth equation

Actual leaf growth is derived from the amount of assimilates available for growth and the death rate of leaves by senescence (Bouman *et al*., 1996a). Leaf senescence is calculated by means of a relative death rate, which is computed from the leaf area index and the ratio of the actual transpiration over the potential transpiration. A high leaf area index leads to internal shading of the lower leaves, which results in leaf senescence. Leaf area development is also affected by grassland management – for example, mowing. In Lingra, two standard management options

are implemented (to be selected by the user): periodic mowing and mowing at a constant biomass level (Bouman *et al*., 1996b).

LAI influences the water balance equation by way of both transpiration and interception. Water demand for transpiration varies throughout the calendar year, peaking during summer, when *LAI* increases, and reducing during winter, when it decreases. Vegetation growth rate, here defined by leaf growth, is calculated as shown in the following equation.

$$2.\quad \Delta LAI = SLA \times f_{(\mathrm{lv})} \times \Delta W - \Delta LAI_{\mathrm{d}}$$

where ΔLAI is the *LAI* increase; *SLA* is the specific leaf area (m^2/g); $f_{(\mathrm{lv})}$ is the fraction of dry vegetation matter to leaves (−); ΔW is the growth rate of crop dry (solid) matter ($(g/m^2)/d$); and ΔLAI_{d} is the death rate of leaf area ($(m^2\ \mathrm{leaf}/m^2\ \mathrm{ground})/d$).

Geotechnical model

The commercial finite-element code, PLAXIS 2D (Plaxis BV, 2018), was used in this study. This geotechnical model is discretised with 15-noded plane-strain triangular elements. The workflow is controlled by way of the PLAXIS Python interface.

Hydromechanical analysis

A fully coupled flow-deformation analysis is used to simultaneously simulate pore water pressure (p_{wp}) and displacements of the dike under transient (saturated and unsaturated) flow conditions. The coupled formulation is based on Biot's theory (Biot, 1941), which includes the equilibrium equation and the continuity equation of the soil–water mixture. Stress equilibrium and Richards' equation (Richards, 1931) are used to govern the mechanical and hydraulic behaviours, respectively, with an extended effective stress used in the mechanical equation. Richards' equation can be used to describe unsaturated flow in a porous medium as

$$3.\quad \boldsymbol{q} = \frac{k_{\mathrm{rel}}}{\rho_{\mathrm{w}}\boldsymbol{g}}\mathbf{k}_{\mathrm{sat}}\left(\nabla p_{\mathrm{wp}} + \rho_{\mathrm{w}}\boldsymbol{g}\right)$$

where $\boldsymbol{q}$ is the vector of specific discharge; $\mathbf{k}_{\mathrm{sat}}$ is the saturated hydraulic conductivity matrix; ρ_{w} is the water density; ∇p_{wp} is the gradient of the pore water pressure that causes the water to flow; $\boldsymbol{g}$ is the vector of gravitational acceleration; and k_{rel} is the relative permeability, defined as the ratio of the hydraulic conductivity at a given saturation to $\mathbf{k}_{\mathrm{sat}}$ (Galavi, 2010). The Mohr–Coulomb constitutive model is used to govern the mechanical behaviour, and the van Genuchten–Mualem model (van Genuchten, 1980) is used to govern the suctions developed from the changes in water content. The van Genuchten–Mualem model is defined as

$$4.\quad \theta = \theta_{\mathrm{r}} + (\theta_{\mathrm{sat}} - \theta_{\mathrm{r}})(1 + |\alpha h|^{n})^{m}$$

where θ is the water content at a given suction h; θ_{r} is the residual water content; θ_{sat} is the water content at saturated conditions; n and m are soil water characteristic curve fitting parameters; and α is a parameter related to the air entry value.

Safety analysis

To obtain the *FoS* variation with time, a safety analysis was performed at various (user-defined) time steps after the coupled analysis. The strength reduction technique was employed to calculate the *FoS* against macro-instability, where the shear strength parameters $\tan\phi$ and c of the soil are successively reduced until failure of the structure occurs (Plaxis BV, 2018); the ratio of the parameters at failure to the defined parameters gives the FoS.

$$5.\quad \mathrm{FoS} = \frac{\tan\phi_{\mathrm{input}}}{\max(\tan\phi_{\mathrm{reduced}})} = \frac{c_{\mathrm{input}}}{\max(c_{\mathrm{reduced}})}$$

where ϕ_{input} and ϕ_{reduced} (c_{input} and c_{reduced}) are the input and reduced friction angles (cohesion), respectively. Bishop's stress is utilised, where suction is included into effective stress, and therefore suction increases shear strength. A single *FoS* is calculated for the entire dike. Other failure mechanisms, such as piping or uplift, are not included in this assessment, nor is there a possibility of a cracking of the dike surface and consequential changes in strength and permeability.

Coupling crop and geotechnical models

The coupling between the crop model and the geotechnical model is shown in Figure 2. The geotechnical model does not include effect of vegetation, so the crop model is used to simulate the growth and decay of vegetation in response to meteorological forcing and the available water amount in the root zone. The flux (Q_{net}) that is applied to the surface boundary in the geotechnical model is defined as

$$6.\quad Q_{\mathrm{net}} = P - In - ET$$

and a zero pore pressure boundary condition is applied on the base.

To ensure that the root zone moisture dynamics are consistent between the two models, the hydraulic parameters in the root zone of the geotechnical model are optimised to ensure that the drainage from the root zone in the crop model (D_L) is equal to that from the 1D geotechnical model (D_P). At each time step, the hydraulic parameters are optimised to minimise the root mean square difference (RMSD) between D_L and D_P.

$$7.\quad F(k_{\mathrm{sat}}, \alpha, n, m) = \min[\mathrm{RMSD}(D_L, D_P)]$$

A 2D hydromechanical model is then used to calculate pore water pressure (p_{wp}) and displacement over time. Finally, the safety

calculation is carried out as described in the previous section to produce the *FoS* against macro-instability as a function of time.

Case study

Two experiments were performed. In the first, 4 years of climatic data were used to obtain the *FoS* time series from 2009 to 2012 to understand the influence of meteorological conditions on the dike safety. Second, to understand the effect of vegetation alone, a single year was simulated for different (fixed) values of *LAI* over that year.

Geometry

The dike geometry used is representative of a regional dike in Amsterdam, the Netherlands, studied in the Veenderij project (de Vries, 2012) and is shown in Figure 1. The vegetation employed in this paper is grass cover with a permanent root depth of 40 cm, equal to the maximum root depth for the considered vegetation (Table 1).

Meteorological data

Meteorological data, such as precipitation (P), solar radiation, average air temperature, wind speed and vapour pressure taken in the early morning at Schiphol airport (Amsterdam) station (52° 19′ 04° 47′ OL), have been obtained from the Royal Netherlands Meteorological Institute for 2009 to 2012 (Figure 4). These data are used as inputs for the crop model.

Root zone: crop model

The key parameters required by the crop model for both soil and vegetation are shown in Table 1. The values are typical for Dutch soil conditions and typical grass cover, based on reported values by Bouman *et al*. (1996a). The listed parameters are divided into two groups, soil and vegetation parameters. In soil parameters, water content field capacity (θ_{fc}) is the maximum water storage capacity of the root zone, which is defined as the volumetric water content at a soil moisture suction of 10 kPa or pF 2·0. The water content at field capacity is therefore lower than water content at saturation (van Laar *et al*., 1997). The water content at the wilting point (θ_{wp}) is the limit of water content, below which plant water uptake ceases and plants start to wilt. Below the critical water content (θ_{cr}), transpiration is reduced by water stress. Drainage is limited by the maximum drainage rate (D_{rate}) of the subsoil. Perennial ryegrass is considered as the vegetation cover and has the majority (85%) of its root system in the shallow soil layer of 0–40 cm below soil surface (Bouman *et al*., 1996b); therefore, the root depth for this permanent grassland is considered fixed at 40 cm. The *SLA* (leaf area/leaf mass) determines how much new leaf area to deploy for each unit of biomass produced. The critical leaf area beyond which death due to self-shading occurs is defined as LAI_{cr} (Wolf, 2006).

Geotechnical model

The sample dike includes two types of soils: the root zone, in which properties should be consistent with the crop model, and the soil of the dike body. Constitutive and hydraulic parameters for the two mentioned parts of the dike are shown in Table 2. The values are based on the default soil properties from the PLAXIS library for the root zone (silt clay) and for the dike body (organic clay), except for the hydraulic values of the root zone which are obtained from the optimisation code.

Table 1. Input parameters used for the crop model

Lingra	Parameter	Value
Soil	θ_{fc}: cm^3 water/cm^3 soil	0·29
	θ_{wp}: cm^3 water/cm^3 soil	0·12
	θ_{cr}: cm^3 water/cm^3 soil	0·005
	D_{rate}: mm/d	50
Vegetation	$d_{M\ root}$: cm	40
	SLA: m^2/g	0·025
	Remaining *LAI* after cutting (LAI_c): m^2 leaf/m^2 ground	0·8
	LAI_{cr}: m^2 leaf/m^2 ground	4

Table 2. Input parameters used for the geotechnical model

	Root zone	Dike body
Constitutive model (Mohr–Coulomb)		
Saturated unit weight, γ_{sat}: kN/m^3	20	12
Friction angle, ϕ: °	23	23
Cohesion, c: kPa	2	2
Dilatancy angle, ψ: °	0	0
Young's modulus, E: MPa	10	20
Initial void ratio, e_{int}	0·67	1·2
Hydraulic model (van Genuchten)		
Permeability, k_{sat}: m/d	0·14	0·03
Scale parameter α: m^{-1}	1·47	1·38
Fitting parameter n	1·97	1·32
Fitting parameter m	0·87	–1·24

Results and discussion

Time series of the SVA interaction variables

Figures 5(a)–5(d) show the temporal pattern of crop model outputs: *LAI*, boundary net flux (Q_{net}), root zone water content (WC_{rz}) and drainage (D_L); and in Figures 5(e)–5(g), the geotechnical model outputs are shown: pore water pressure (p_{wp}), magnitude of displacement and FoS, in the example dike from 2009 to 2012.

The *LAI* values in Figure 5(a) reflect seasonal dynamics. *LAI* is highest in spring and summer, since vegetation growth is energy-limited rather than water-limited. Reduced solar radiation limits growth in the autumn and winter. Higher *LAI* values in the summer lead to higher evapotranspiration and hence a reduction in the amount of water flux into the dike. The sudden decreases in *LAI* on 15 June and 15 August are due to grass mowing. These mowing events were imposed based on the mowing schedule for regional dikes in the Netherlands (T. Reuzenaar, 2017, private communication).

In Figure 5(b), positive Q_{net} values occur in response to precipitation events. On days with near-zero precipitation and

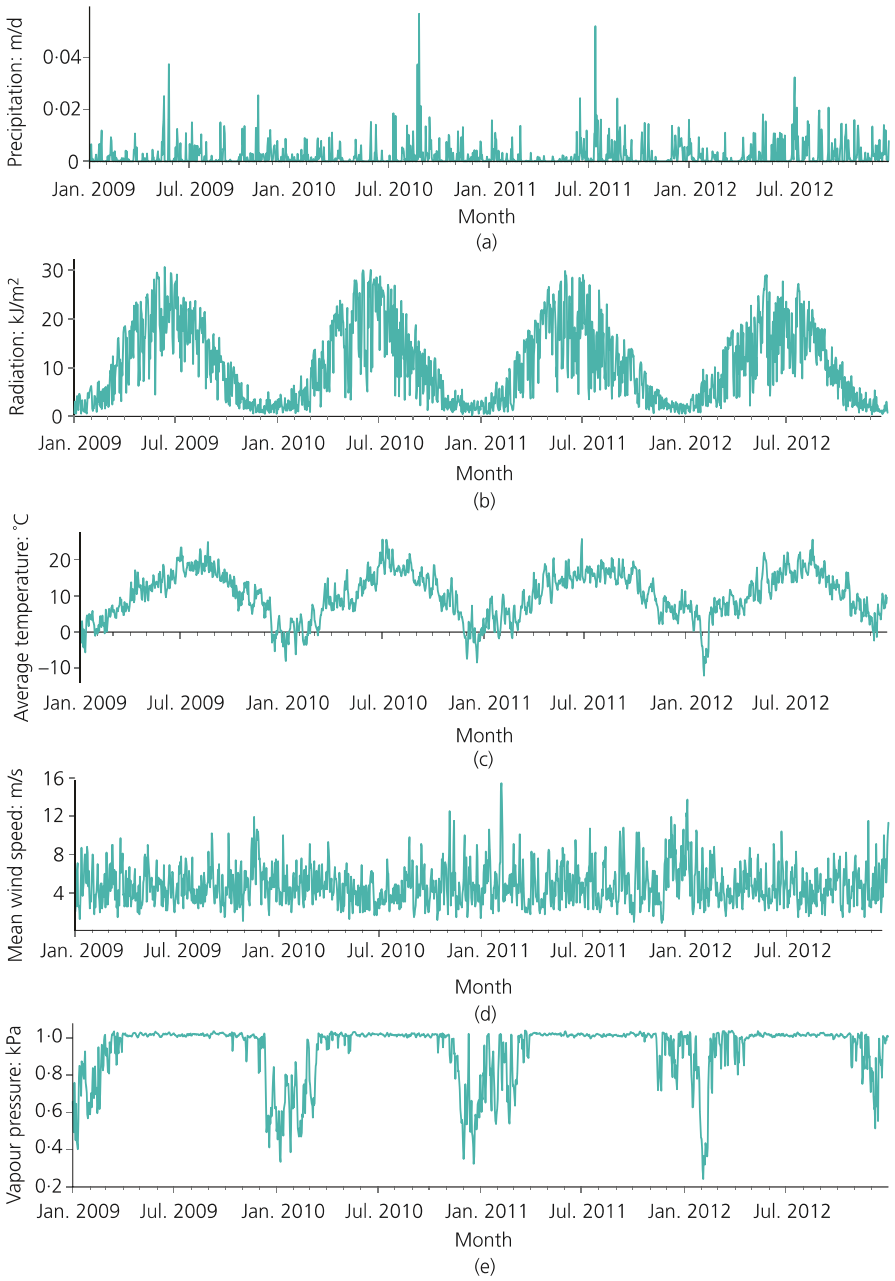

Figure 4. Daily values of inputs for the crop model from 2009 to 2012: (a) precipitation; (b) radiation; (c) average temperature; (d) average wind speed; (e) vapour pressure in the early morning

high LAI, Q_{net} is negative as evaporative demand exceeds precipitation and then moisture in the root zone decreases – for example, in April and May 2011.

In Figure 5(c), the water content in the root zone is seen to decrease during the summer due to high levels of evapotranspiration. It follows that during periods with a consistently high Q_{net}, the root zone reaches the field capacity. At this moment drainage is able to occur. Drainage to the dike body (D_L) is shown in Figure 5(d). As seen in Figures 5(b) and 5(c), drainage occurs when there is a positive (downward) Q_{net} and WC_{rz} reaches the field capacity. This can generally be seen in the winter months. A spike is also apparent in August 2010 when a large precipitation event occurred while LAI was low.

In Figure 5(b), the maximum Q_{net} during these 4 years is in August 2010 (0·055 m/d), which leads to the maximum D_L (0·034 m/d). However, the second largest Q_{net}, 0·049 m/d, is in July 2011, and it does not cause any drainage on the same day (Figure 5(d)). This comes from the fact that there is more available storage in the root zone in the latter day (WC_{rz} = 0·16 (cm^3 water/cm^3 soil)) relative to the former one (WC_{rz} = 0·23 (cm^3 water/cm^3 soil)), as shown in Figure 5(c). More limited drainage does occur in the days after the large rainfall in July 2011 due to additional rainfall and the saturated root zone.

In Figure 5(e), the pore water pressure (p_{wp}) at points A and B is shown. Positive and negative indicate pressure and suction, respectively. Comparing Figures 5(d) and 5(e), it is clear that drainage from the root zone increases p_{wp}. High drainage (August 2010), or long periods of cumulative drainage (winter 2009–2010), leads to higher p_{wp} (soil is saturated) at points A and B. As expected, when the WC_{rz} decreases (e.g. during the spring), p_{wp} decreases. The highest suction (negative p_{wp}) is observed at points A and B during the very dry spring of 2011.

Comparing Figures 5(d)–5(f), it is clear that drainage into the dike body increases p_{wp}, which in turn increases (upwards) the magnitude of displacement at points A and B. The displacement peaks following large precipitation events and recovers between events, showing a mainly elastic response. A slight accumulation of displacement over time is observed, due to plastic displacement.

In Figure 5(g), temporal variation of *FoS* is shown, which derived from the combined effect of precipitation and *LAI* that influence Q_{net}. A similar temporal pattern can be seen, as exhibited in Figures 5(f) and 5(g). The largest decrease in *FoS* corresponds to the maximum drainage, in August 2010, while during dry periods when suction increases, the *FoS* tends to increase as well – for example in March–May 2011. However, the relation is not fully proportional and further investigation is needed. It is noted that in extremely dry conditions, cracking in the surface of the dike could occur. This is not taken into account in the model.

Figure 5(h) shows the phreatic line of the dike on two selected days. The sub-figure on the left represents a day where the dike is in a dry condition (in June 2011) with a very low WC_{rz}, thereby also a low p_{wp} and high *FoS*. In comparison, on the right is a sub-figure representing the dike in a wet condition (in July 2011) in which the saturation increased and the phreatic line rises in the soil body and reaches the surface on the downstream side.

In Figure 6, the predicted failure mode is shown for the wet day mentioned earlier. The failure is circular, and it fails into the water-retaining side due to the asymmetric geometry of the dike.

WC_{rz} influence on *FoS*

In order to study how the soil water content in the root zone influences the dike safety, *FoS* values are plotted against WC_{rz} in Figure 7. During the simulated period, results suggest that a drier root zone (lower WC_{rz}) leads to higher safety in the dike. This was expected, since the drier root zone leads to higher suction and then higher strength. However, it is also clear that it is not a unique relationship.

To understand *LAI* effect on the SVA interaction, the results in Figure 7 are shaded by *LAI*, with values increasing from white (low *LAI*) to black (high *LAI*). It can be seen that, generally, a dry root zone leads to low *LAI* values; however, low *LAI* does not correspond to low values of WC_{rz} in mowing and winter times. The minimum *FoS* values seem to occur at a mid-range value of *LAI* and high WC_{rz}, probably caused due to high antecedent water content, which leads to increased grass growth, but with a limited evapotranspiration rate (caused at high *LAI* values). Neither WC_{rz} nor *LAI* has a unique relation with *FoS*, despite the strong trend.

Correlation among selected SVA variables

Correlation coefficients between pairs of key variables have been calculated considering time and are presented in Figure 8. If the maximum absolute value of correlation occurs with a positive lag, it means that the second term leads the first. If the peak correlation value occurs at a negative lag, then the first term leads the second one.

The peak correlation coefficient between *LAI* and WC_{rz} (r = 0·31) (Figure 8(a)) is obtained with a 15 d lag, which means WC_{rz} affects *LAI* the most after 15 d. This reflects that the vegetation grows in response to water content availability. The weak, although positive, correlation increases from a lag of −30 d, reaching a maximum at 15 d, and is still positive after 30 d. It is due to the fact that *LAI* is a result of WC_{rz} over a relatively long time. The amount of water in the root zone is not the only factor which influences the *LAI*, mowing and radiation have key roles in vegetation growth.

The correlation between WC_{rz} and *FoS* (Figure 8(b)) is negative, with no time lag. This agrees with the previous physical argument that more available water in the root zone increases the mass of the dike (and the overturning moment) and decreases the strength.

In contrast to WC_{rz}, there is a generally positive correlation between *LAI* and *FoS*, with a 15 d lag, which is shown in Figure 8(c). A high *LAI* results in increased transpiration, leaf interception and reduced drainage into the dike (see next section).

In Figure 8(d), the correlation coefficient between the water content in the dike body (WC_{body}) and *FoS* is plotted, which has the strongest correlation of all of the considered parameters. The water content in the dike body is calculated as a spatial average of the whole body. It is shown that a higher WC_{body} leads to a lower *FoS* with no time lag; in other words, they are negatively correlated. As with the water content in the root zone, the increased weight and reduced strength with an increase in water content is the cause of the negative correlation.

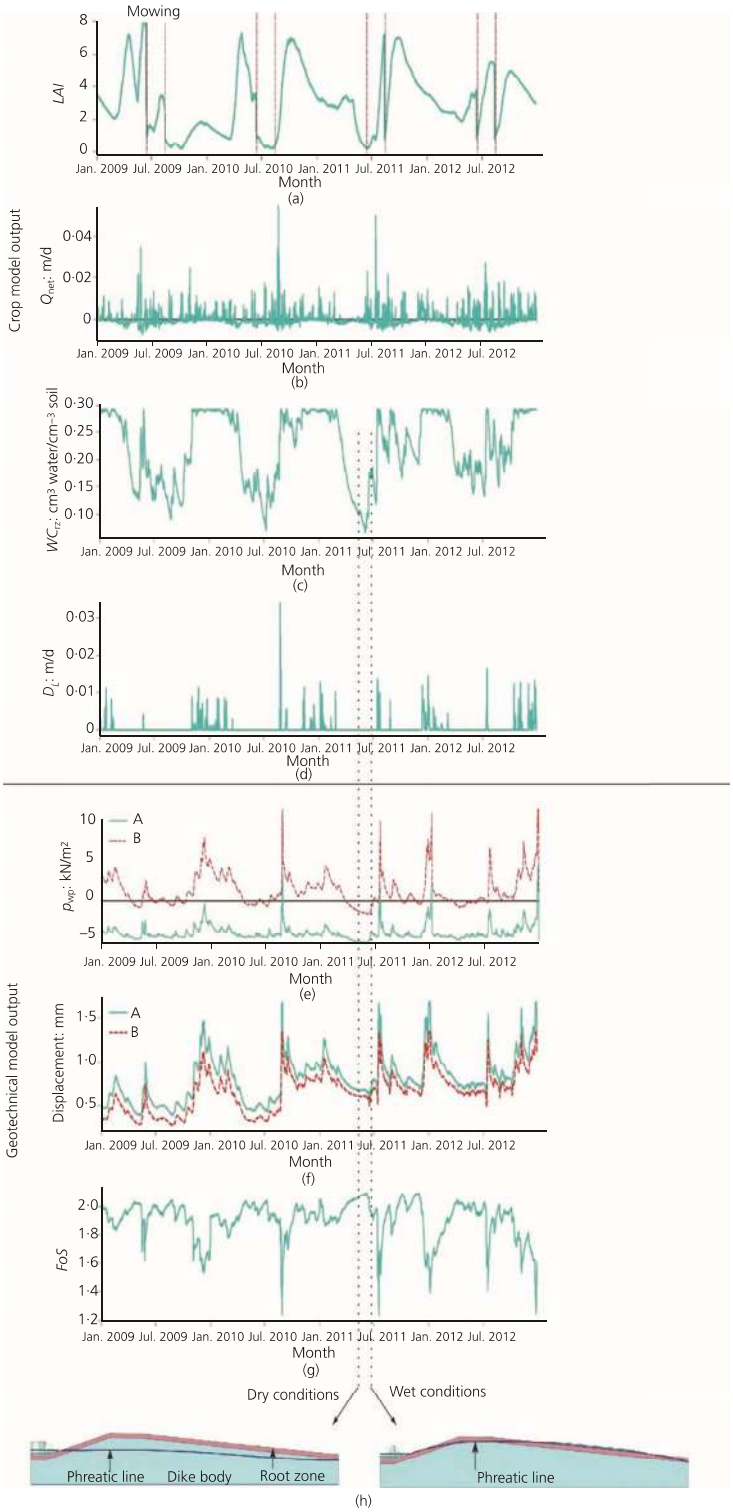

Figure 5. Daily values of (a) LAI; (b) boundary net flux (Q_{net}); (c) root zone water content (WC_{rz}); (d) drainage from root zone to lower layers (D_L); (e) pore water pressure (p_{wp}) at points A and B (compression is positive); (f) magnitude of displacement at points A and B and (g) *FoS*, over 4 years; (h) phreatic line in a dry and wet condition

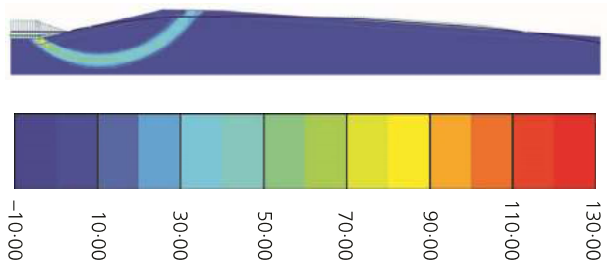

Figure 6. Deviatoric strain predicted during the failure calculation on the wet day, representing the failure mode

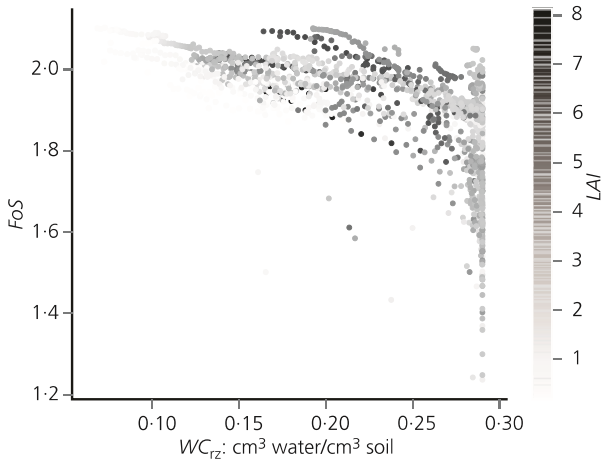

Figure 7. The *FoS* plotted against the water content in the root zone (WC_{rz}) during a simulation of four years. Points are shaded by *LAI*

Water moves downwards through the dike, reducing effective stress and thereby also reducing the strength; after water has passed through the dike, if there is no further rain, the strength can recover. In the conditions when the ratio of shear strength to shear stress is the lowest, the dike may fail.

Drainage from the root zone into the dike body causes a decrease in *FoS* in the same day (Figure 8(e)). D_L is the key driver for WC_{body}, drainage variations makes WC_{body} change, which then negatively affects *FoS* (Figure 8(d)).

LAI effect

As discussed in the previous section, *LAI* varies due to multiple reasons including radiation, precipitation, root zone water content and mowing. Hence, it is difficult to explore the impact of solely the vegetation. To study the impact of *LAI*, different constant values have been selected and the simulation re-run for a single year – that is, 2010.

Figure 9(a) shows the precipitation over the year, and in Figure 9(b), cumulative boundary net flux (see Equation 6) is plotted to describe how *LAI* affects Q_{net}. The differences between the values of Q_{net} stem solely from the differences in *LAI* – that is, changes in evapotranspiration and leaf interception. Higher values of *LAI* lead to higher plant transpiration and leaf interception rate, but lower evaporation. As presented in Figure 9(b), the case with no vegetation yields the highest Q_{net} throughout the whole year. The impact on *FoS* for 2010 is shown in Figure 9(c). Since Q_{net} for $LAI = 0$ and $LAI = 1$ is very similar, the safety calculation has been done only for the latter case. As expected, the wetter the dike (higher Q_{net}), the lower the *FoS*. This occurs with a lower *LAI*, and so less vegetation causes lower *FoS*, whereas the case with the highest *LAI* generally leads to higher *FoS* over the year. This argument proves the positive correlation between *LAI* and *FoS* which has been shown in Figure 8(c).

In a nutshell, presence of vegetation improves the safety of a dike since it decreases the water that reaches the root zone and consequently dike body. If *LAI* is 1, it represents a very patchy vegetation and almost bare soil, and it is seen that in this case *FoS* generally is less than the other two cases. This demonstrates the importance of including vegetation in regional dike analysis.

The possibility of using vegetation as a safety indicator

Vegetation is strongly coupled to the moisture available in a dike and particularly in the root zone. Other meteorological aspects also govern this value; therefore, a seasonal change is also seen. The vegetation responds to moisture in the root zone, which means that the vegetation follows the precipitation (most strongly after 15 d); therefore, it is likely that it could be used as an indicator of safety. Additionally, the lagged correlation between *LAI* and *FoS* means that it may be possible to utilise *LAI* as a predictive tool. Reduced *LAI* will increase boundary net flux (Q_{net}) and reduce *FoS*.

What is attractive is that the vegetation could quite easily be monitored remotely – that is, by way of satellites or drones, rather than having to install physical sensors, which are extremely expensive with a limited coverage. A complicating factor is dike maintenance – that is, mowing, which dramatically alters *LAI* over a very short period of time, as well as the complex history-dependent factors that affect *LAI* and *FoS*. With a knowledge of the meteorological conditions, maintenance and the evolution of the vegetation, it may be possible to carry out history matching modelling on identified vulnerable areas to give a better insight into the conditions of the dike. It may be possible to have a staged process, where (*a*) vulnerable dikes are identified, using vegetation and root zone water content monitoring; (*b*) numerical history matching is carried out to identify at-risk dikes; and (*c*) the at-risk dikes are physically inspected. In each stage, a more limited length of dike is considered.

One limitation of this work is the lack of consideration of surface cracking of the soil, which occurs in very dry conditions. Vegetation has been observed to reduce around cracks (e.g Hasan *et al.* (2013)), probably due to enhanced drainage and

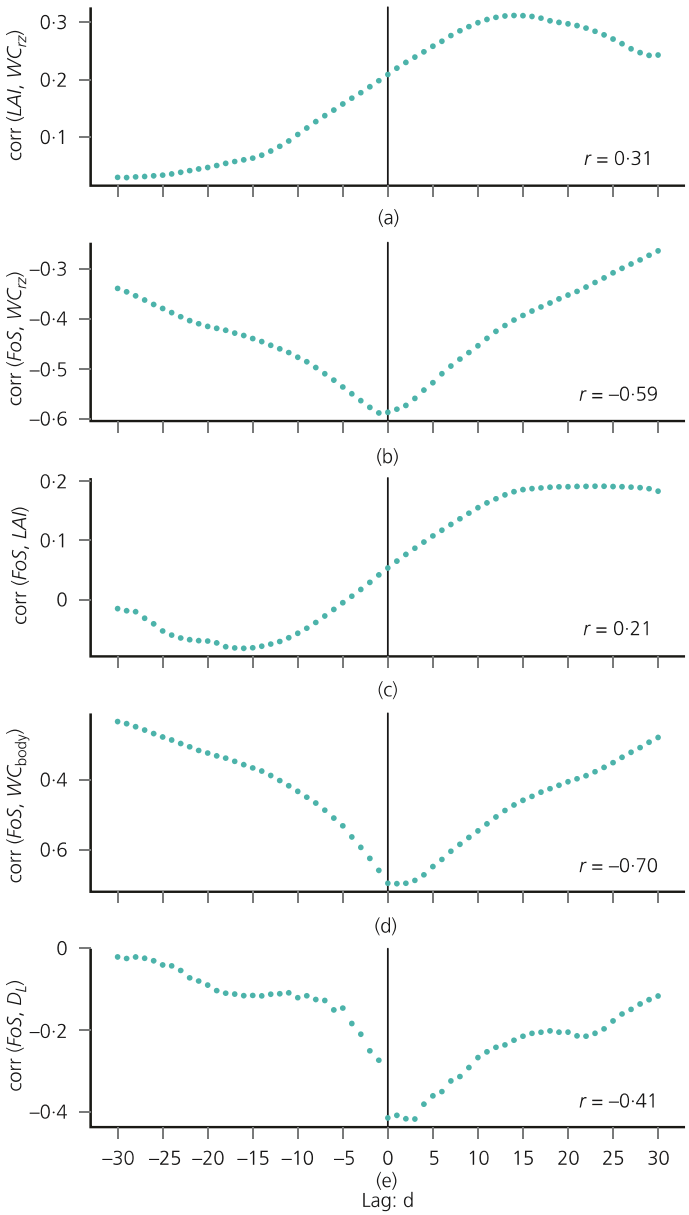

Figure 8. Correlation coefficient (r) between (a) leaf area Index and root zone water content; (b) factor of safety and root zone water content; (c) factor of safety and leaf are index; (d) factor of safety and average water content in dike body; (e) factor of safety and drainage from root zone with time lags up to 30 d during 4 years. A positive lag means that the second variable leads the first

evaporation. A lower *LAI* in this case will also indicate a weaker dike but for different reasons that are previously discussed. The history matching will be complicated by this aspect.

To the authors' knowledge, neither comprehensive field nor laboratory data are available to validate this numerical research, and it is suggested for future studies. The individual components that have been used in this study, Lingra and PLAXIS, are validated by Schapendonk *et al*. (1998) and Plaxis BV (2018).

Conclusion and discussion

In this paper, the SVA interaction of an example dike covered with grass is investigated along with how this interaction governs the dike's hygroscopic condition and macro-stability. Two numerical models, a crop model and a geotechnical model, were coupled together to simulate SVA interaction over a period of 4 years. In the current study, the impact of surface cracking of the soil is not considered and the approach is yet to be validated with experimental data. It is shown that the amount of vegetation strongly affects the

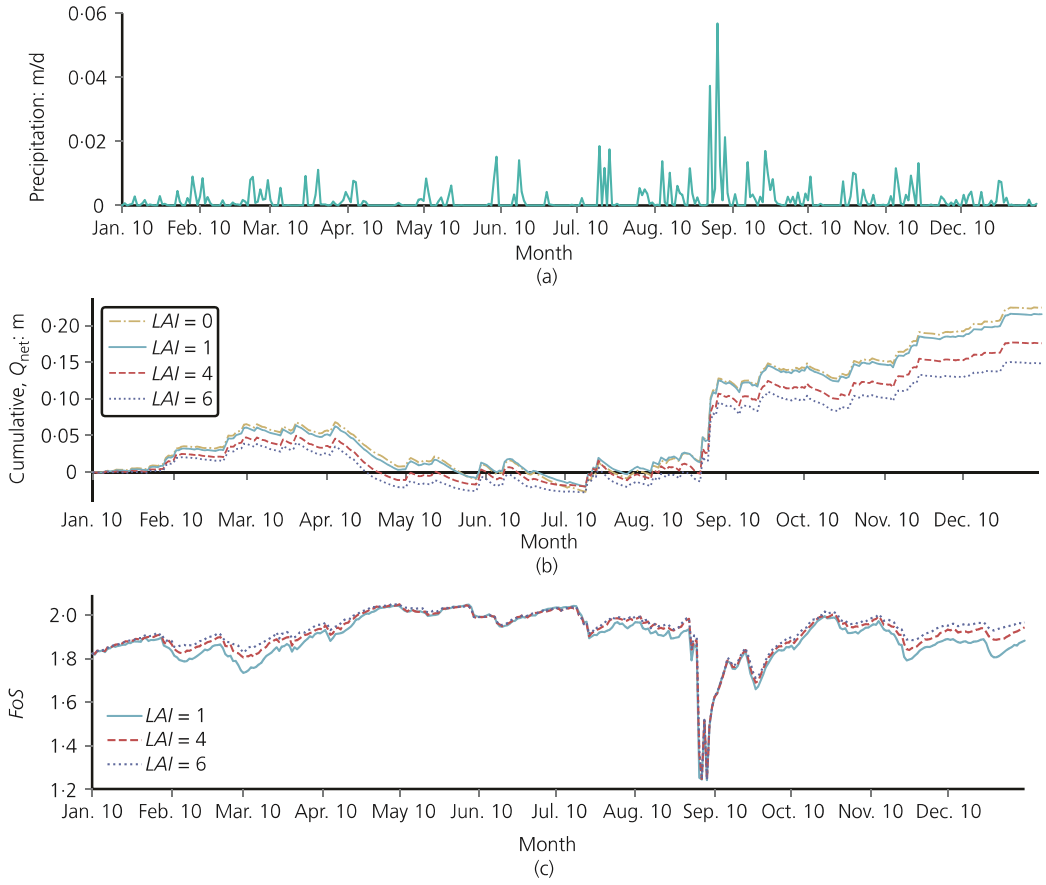

Figure 9. For different constant *LAI*s over 2010: (a) precipitation (m/d); (b) cumulative boundary net flux (m); (c) *FoS*

water flux into the dike and consequently impacts *FoS*. *FoS* is mostly dependent on the water content in both the root zone and the dike body, but that is affected by the vegetation. Moreover, the history of the precipitation and water content have an impact on both *FoS* and the vegetation. It is therefore proposed that vegetation and root zone water content could be used as proxies to detect vulnerable dikes at an early stage.

Acknowledgements

This work is part of the research programme Reliable Dikes with project number 13864, which is financed by the Netherlands Organisation for Scientific Research. The authors would like to thank Dr R. Brinkgreve and Dr V. Galavi for helpful discussions on PlaxFlow analysis.

REFERENCES

Biot MA (1941) General theory of three-dimensional consolidation. *Journal of Applied Physics* **12(2)**: 155–164, https://doi.org/10.1063/1.1712886.

Bouman BAM, Schapendonk AHCM, Stol W and van Kraalingen DWG (1996a) *Description of the Growth Model LINGRA as Implemented in CGMS Quantitative Approaches in Systems Analysis No. 7., DLO Research Institute for Agrobiology and Soil, Wageningen, the Netherlands.*.

CIRIA (Construction Industry Research and Information Association), MEDE (Ministère de l'Ecologie du Développement durable et de l'Energie) and USACE (US Army Corps of Engineers) (2013) *The International Levee Handbook*. CIRIA, London, UK.

Cundill SL (2016) *Investigation of Remote Sensing for Dike Inspection*. PhD thesis, University of Twente, Enschede, the Netherlands.

de Vries G (2012) *Monitoring Droogteonderzoek Veenkaden*. Deltares, Delft, the Netherlands (in Dutch).

Digigids (2016) STOWA, the Netherlands. See http://digigids.hetwaterschapshuis.nl/index.php?album=Grasbekledingen-2019-/gras.

Elia G, Cotecchia F, Pedone G *et al.* (2017) Numerical modelling of slope–vegetation–atmosphere interaction: an overview. *Quarterly Journal of Engineering Geology and Hydrogeology* **50(3)**: 249–270, https://doi.org/10.1144/qjegh2016-079.

Franzluebbers AJ (2011) Stratification of soil porosity and organic matter. *Encyclopedia of Agrophysics*: 858–861, http://dx.doi.org/10.1007/springerreference_224121.

Galavi V (2010) *Groundwater Flow, Fully Coupled Flow Deformation and Undrained Analyses in PLAXIS 2D and 3D*. Plaxis BV, Delft, the Netherlands.

Hasan K, Aanstoos JV and Mahrooghy M (2013) Stressed vegetation identification by SAR time series as an indicator of slope instability in

Mississippi river levee segments. *Proceedings of the 2013 IEE Applied Imagery Pattern Recognition Workshop (AIPR): Sensing for Control and Augmentation, Washington, DC, USA*, pp. 1–4.

Hemmati S, Gatmiri B, Cui YJ and Vincent M (2012) Thermo-hydro-mechanical modelling of soil settlements induced by soil–vegetation–atmosphere interactions. *Engineering Geology* **139–140**: 1–16, https://doi.org/10.1016/j.enggeo.2012.04.003.

Plaxis BV (2018) *PLAXIS Reference Manual 2018*. Plaxis BV, Delft, the Netherlands.

Rahardjo H, Satyanaga A and Leong EC (2013) Effects of flux boundary conditions on pore-water pressure distribution in slope. *Engineering Geology* **165**: 133–142, https://doi.org/10.1016/j.enggeo.2012.03.017.

Richards LA (1931) Capillary conduction of liquids through porous mediums. *Journal of Applied Physics* **1(5)**: 318–333, https://doi.org/10.1063/1.1745010.

Schapendonk AHCM, Stol W, Van Kraalingen DWG and Bouman BAM (1996) Description of LINGRA. In *Description of the Growth Model LINGRA as Implemented in GCMS* (Bouman BAM, Schapendonk AHCM, Stol W and van Kraalingen DWG (eds)). Quantitative Approaches in Systems Analysis No. 7., DLO Research Institute for Agrobiology and Soil Fertility, Wageningen, the Netherlands, pp. 11–22.

Schapendonk AHCM, Stol W, Van Kraalingen DWG and Bouman BAM (1998) LINGRA, a sink/source model to simulate grassland productivity in Europe. *European Journal of Agronomy* **9(2–3)**: 87–100, https://doi.org/10.1016/s1161-0301(98)00027-6.

Shibu ME, Leffelaar PA, Van Keulen H and Aggarwal PK (2010) LINTUL3, a simulation model for nitrogen-limited situations: application to rice. *European Journal of Agronomy* **32(4)**: 255–271, https://doi.org/10.1016/j.eja.2010.01.003.

Spitters CJT (1987) An analysis of variation in yield among potato cultivars in terms of light absorption, light utilization and dry matter partitioning. *Agrometeorology of the Potato Crop* **214**: 71–84, https://doi.org/10.17660/actahortic.1988.214.5.

TAW (Technical Advisory Committee for Flood Defence) (1996) *Clay for Dikes*. Road and Hydraulic Engineering Institute, Delft, the Netherlands.

Tsiampousi A, Zdravkovic L and Potts DM (2016) Numerical study of the effect of soil–atmosphere interaction on the stability and serviceability of cut slopes in London clay. *Canadian Geotechnical Journal* **54(3)**: 405–418, https://doi.org/10.1139/cgj-2016-0319.

van Genuchten MT (1980) A closed-form equation for predicting the hydraulic conductivity of unsaturated soils. *Soil Science Society of America Journal* **44(5)**: 892–898, https://doi.org/10.2136/sssaj1980.03615995004400050002x.

van Laar HH, Goudriaan J and van Keulen H (1997) *SUCROS97: Simulation of Crop Growth for Potential and Water-Limited Production Situations. As Applied to Spring Wheat*. Quantitative Approaches in Systems Analysis No. 7., DLO Research Institute for Agrobiology and Soil Fertility, Wageningen, the Netherlands.

Vardon PJ (2015) Climatic influence on geotechnical infrastructure: a review. *Environmental Geotechnics* **2(3)**: 166–174, https://doi.org/10.1680/envgeo.13.00055.

Wolf J (2006) *Grassland Data from PASK Study and Testing of LINGRA in CGMS*. Alterra, Wageningen, the Netherlands. Asemars Project Report No. 2.

How can you contribute?

To discuss this paper, please submit up to 500 words to the editor at journals@ice.org.uk. Your contribution will be forwarded to the author(s) for a reply and, if considered appropriate by the editorial board, it will be published as a discussion in a future issue of the journal.